Accepted Manuscript

Author: Eliana Sousa Da Silva Mohamed Sarakha Hugh D. Burrows Pascal Wong-Wah-Chung

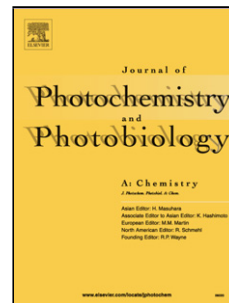Please cite this article as: Eliana Sousa Da Silva, Mohamed Sarakha, Hugh D.Burrows, Pascal Wong-Wah-Chung, Decatungstate anion as an efficient photocatalytic species for the transformation of the pesticide 2-(1-naphthyl)acetamide in aqueous solution, Journal of Photochemistry and Photobiology A: Chemistry http://dx.doi.org/10.1016/j.jphotochem.2016.10.036

This is a PDF file of an unedited manuscript that has been accepted for publication. As a service to our customers we are providing this early version of the manuscript. The manuscript will undergo copyediting, typesetting, and review of the resulting proof before it is published in its final form. Please note that during the production process errors may be discovered which could affect the content, and all legal disclaimers that apply to the journal pertain.

Decatungstate anion as an efficient photocatalytic species for the transformation of the pesticide 2-(1-naphthyl)acetamide in aqueous solution

Eliana Sousa Da Silva,[a,b,c,1] Mohamed Sarakha,[a,c] Hugh D. Burrows[b] and Pascal Wong-Wah-Chung[e*]

[a]*Clermont Université, Université Blaise Pascal, Institut de Chimie de Clermont Ferrand (ICCF) UMR CNRS 6296, Équipe Photochimie, BP 80026, F-63171 Aubière Cedex, France*

[b]*Centro de Química, Department of Chemistry, University of Coimbra, Rua Larga, 3004-535, Coimbra, Portugal*

[c]*CNRS, UMR 6505, 24 avenue des Landais, F-63173 Aubière, France*

[d]*Clermont Université, ENSCCF, BP 10448, F-63000 Clermont-Ferrand, France*

[e]*Aix Marseille Univ, CNRS, LCE, Marseille, France*

[1]*Present affiliation: Laboratory of Separation and Reaction Engineering – Laboratory of Catalysis and Materials (LSRE–LCM), Departamento de Engenharia Química, Faculdade de Engenharia, Universidade do Porto, Rua Dr. Roberto Frias s/n, 4200-465 Porto, Portugal*

*Corresponding author: E-mail addresses: pascal.wong-wah-chung@univ-amu.fr, (P. Wong-Wah-Chung), Tel: +033 4 42 90 84 16; fax: +033 4 91 28 84 27, elianas@qui.uc.pt (E.S. Da Silva), mohamed.sarakha@univ-bpclermont.fr (M. Sarakha), burrows@ci.uc.pt (H.D. Burrows)

GRAPHICAL ABSTRACT
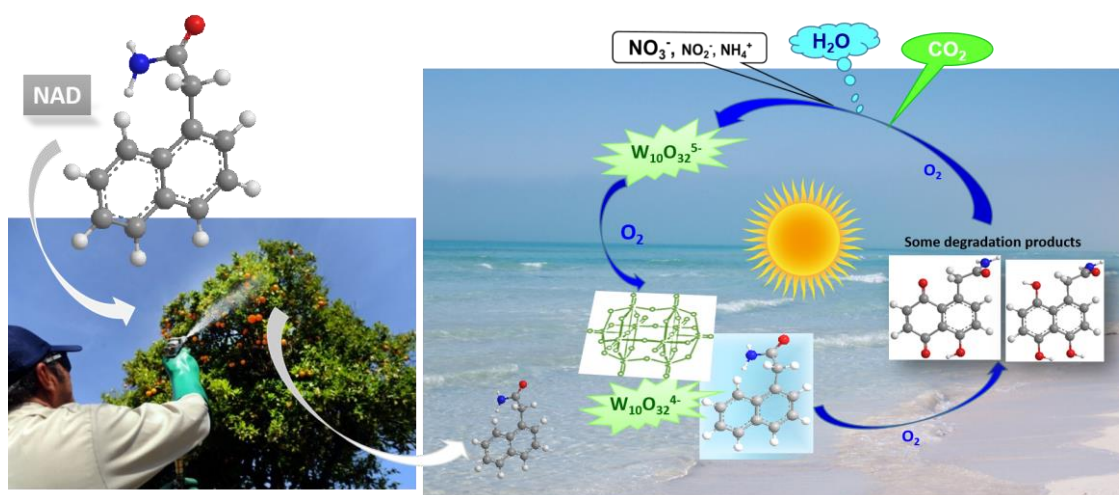
Highlights

- $W_{10}O_{32}^{4-}$ is effective on the photodegradation of the pesticide 2-(1-naphthyl)acetamide (NAD).
- NAD degradation is enhanced in the presence of the catalyst $W_{10}O_{32}^{4-}$ when compared to its direct degradation.
- $W_{10}O_{32}^{4-}$ efficiently promotes NAD mineralization to CO_2, H_2O, NO_3^-, NO_2^- and NH_4^+.
- Oxygen is crucial to regenerate the catalyst $W_{10}O_{32}^{4-}$, thus closing the photocatalytic cycle.
- The first step of the photodegradation probably corresponds to an electron transfer process.
- Hydroxylation and oxidation products were identified. No reactivity of NAD amide side chain was observed.

Abstract

The degradation and mineralization of the plant growth regulator 2-(1-naphthyl)acetamide (NAD) was studied by excitation of the catalyst polyoxometalate decatungstate anion ($W_{10}O_{32}^{4-}$) in aqueous solution under UV (365 nm) and simulated solar light exposure. Our results indicate that the photocatalytic degradation of NAD is dependent on molecular oxygen concentration: in aerated conditions, 95% degradation was achieved after 22 h irradiation, and followed first-order kinetics with a rate constant of 3.2×10^{-3} min^{-1}, while under de-aerated conditions almost no degradation was observed (6.0% after 22 h). Upon UV irradiation, the catalyst $W_{10}O_{32}^{4-}$ enhanced NAD photodegradation by a factor of about 20 compared to its direct degradation. Oxygen appeared to play a key role on the regeneration of the catalyst, promoting the photocatalytic cycle. The primary photoproducts of NAD photocatalytic degradation were assessed by LC-ESI-MS/MS, from which a mechanism of degradation involving electron transfer and hydrogen atom abstraction is proposed. Under these conditions, mono- and di-hydroxylated and oxidized products similar to those obtained under direct photolysis have been identified. In addition, tri-hydroxylation and hydroxyl-naphthoquinone products have been identified exclusively when photolysis was carried out in presence of this catalyst. For prolonged photolysis times, it is expected that the irradiation of the tri-hydroxylated products leads to the opening of the aromatic ring and to mineralization. Furthermore, mineralization was achieved, with the formation of the inorganic ions NO_2^- (< 6.0 µg L^{-1}), NO_3^- (2.6 mg L^{-1}) and NH_4^+ (< 0.5 µg L^{-1}).

1. Introduction

The extensive use of pesticides in agriculture and in urban environments has contributed in recent years to their ubiquitous presence in surface and groundwater [1, 2]. Owing to their nature, most pesticides are persistent in the environment due to their resistance to chemical and/or photochemical degradation [3, 4]. They may build up in animal tissues, as well as contaminating food and drinking water, with the consequent serious threat to human and animal health [5-9]. The pesticide 2-(1-naphthyl)acetamide, hereafter designated as NAD, (Fig. 1), belongs to the family of plant growth regulators. It is applied in agriculture as a component in many commercial plant rooting and horticultural formulations (*Amid-Thin W*, *Amcotone*, etc.) with the goal of improving the growth of fruits (apple, pear, peach, grape, etc.), as well as preventing their drop shortly before harvest [10-12]. The use of plant growth regulators to decrease pre-harvest abscission on citrus fruits was first reported in 1941 by Gardner [13]. He discovered that the application of NAD to pineapple oranges early in the harvest season at a concentration of 100 mg L^{-1} reduced fruit drop for twelve weeks or longer [13]. However, NAD is considered harmful to aquatic organisms, with a LC_{50} of 44 mg L^{-1} for fish, and a half-life of 38 days in water [10]. Its prolonged application in agriculture over the last few years makes it a potential water pollutant [10, 12].

Recently, we reported the direct photolysis of NAD in aqueous solution under UV and simulated solar light exposure [14]. Under these conditions, the photochemical transformation of NAD mainly involves the aromatic moieties, without any participation of the amide side chain. Mono- and di-hydroxylated NAD derivatives, as well as oxidation products, such as naphthoquinone, furanone and coumarin derivatives, were identified as the primary photoproducts. The effect of the irradiation on NAD toxicity was also assessed, and a direct correlation was drawn between the increase in toxicity and the formation of these primary photoproducts. These results aroused our interest in developing a methodology that is able both to transform NAD photochemically through the use of solar light, and to mineralize it, specifically, by transforming it into environmentally innocuous compounds such as CO_2, H_2O, and nitrogen inorganic compounds.

Advanced oxidation processes (AOPs) [15-20] are among the current methods described in literature that have enormous potential to reduce the impact of these pollutants in the environment, since they can lead to total mineralization, or at least to

their transformation into less harmful products. The AOPs typically use UV and UV-near visible radiation, and/or strong oxidizing agents, which produce highly reactive oxygen species, such as hydroxyl radicals (HO$^\bullet$), superoxide anion (O$_2^{\bullet-}$), etc., that are responsible for the transformation of these organic compounds into less harmful products [15, 19, 20]. Fenton, photo-Fenton, H$_2$O$_2$/UV, O$_3$, O$_3$/UV, O$_3$/UV [21-23], and heterogeneous photocatalysis using semiconductor materials, such as TiO$_2$, CdS, ZnO, WO$_3$, etc. [20, 24-28] are some of the methods reported for water remediation. Although UV/TiO$_2$ is by far the most widely studied system [29-32], another important branch of AOPs developed in recent decades, which also provides promising results for water remediation, involves the use of polyoxometalates (POMs) in the presence of light [33-39]. Comparative studies on the action mode of UV/TiO$_2$ *vs* UV/POMs suggest that POMs present the same photochemical characteristics as TiO$_2$ [40-43], but have, as advantage, their low cost and relatively low toxicity. POMs are well-defined early transition metal-oxygen clusters, with unique electronic versatility, and are able to undergo photoinduced multi-electron transfer, without any change in their structure [44-48]. These characteristics broaden the range of application to fields such as chemistry, biology, medicine, catalysis, photocatalysis and materials science [41, 49-53]. The most frequent application of POMs is probably in the field of catalysis, associated with their attractive redox properties [47, 54, 55]. The decatungstate anion, W$_{10}$O$_{32}^{4-}$, is one of the most photochemically active polyoxometalates, and exhibits attractive properties as a photocatalyst [56, 57], since it possesses a UV absorption spectrum which partially overlaps the UV solar emission spectrum, diminishing the energy consumption through the possible use of solar light [56, 58, 59]. It is established in the literature that the absorption of light by W$_{10}$O$_{32}^{4-}$ leads to the formation of a charge transfer excited state (W$_{10}$O$_{32}^{4-*}$) that decays in approximately 30 ps to a longer-lived, extremely reactive and non-emissive transient, designated as wO (lifetime of 35 ns in water) [60-64]. Such a transient species, which is a relaxed excited state, exhibits oxyradical-like character due to the presence of an electron deficient oxygen center, and does not react with oxygen. However, it reacts extensively with organic substrates, producing radicals through hydrogen atom abstraction or electron transfer mechanisms. In the presence of oxygen, these radicals may lead to the formation of peroxy- compounds [62, 65-67]. Both mechanisms lead to the formation of the one-electron reduced form of decatungstate, W$_{10}$O$_{32}^{5-}$ or its protonated form HW$_{10}$O$_{32}^{4-}$ [47, 68], which regenerates the starting W$_{10}$O$_{32}^{4-}$ in the presence of oxygen [69], completing the catalytic cycle. Such a cycle can

lead to the continuous degradation of organic substrates and to their total elimination, as confirmed by studies concerning the degradation of various types of organic pollutants in water [35, 37, 58, 70-72].

Consequently, based on these photochemical properties of $W_{10}O_{32}^{4-}$, we became interested in assessing the transformation of NAD in the presence of this photocatalyst in aqueous solution under UV and simulated solar light irradiation, with particular attention in evaluating the catalytic activity of $W_{10}O_{32}^{4-}$ on its degradation. This was done by following its degradation and mineralization processes. The disappearance kinetics, initial rate constants and quantum yields of degradation were determined as a function of oxygen concentration. In addition, the degree of mineralization was evaluated through measurement of both the total organic carbon concentration and the inorganic species produced. The primary organic products formed during the photocatalytic degradation were identified, and a mechanism of the photodegradation is proposed. Moreover, a comparison is made regarding the products formed from NAD under normal photolysis and photocatalysed degradation.

2. Materials and methods

2.1. Materials

2-(1-Naphthyl)acetamide (NAD), methanol (Chromasolv, $\geq$ 99.9% for HPLC) and formic acid (reagent grade, $\geq$ 95%) were purchased from Sigma Aldrich, and *iso*-propanol from Riedel-de Haën. Sodium decatungstate ($Na_4W_{10}O_{32}.7H_2O$) was synthesized according to a literature procedure [73], and fully characterized. Ultrapure water, delivered by a Millipore Milli-Q system (18.2 MΩ cm^{-1}; no control of ionic strength), was used throughout this study. Aqueous solutions of the mixture [NAD +$W_{10}O_{32}^{4-}$] were freshly prepared at room temperature by directly dissolving the necessary amount of $Na_4W_{10}O_{32}.7H_2O$ powder in aqueous NAD solution, prior to starting the irradiation. Solutions were de-aerated and oxygenated by bubbling argon and oxygen, respectively, for 30 min prior to irradiation and during the whole irradiation period, when necessary.

2.2. Irradiation systems

For determination of the quantum yields, homogeneous aqueous solutions of NAD in the presence of $W_{10}O_{32}^{4-}$ were irradiated at 365 nm with a LOT Oriel grating

monochromatic system equipped with a xenon lamp (1000 W). The beam was parallel and the reactor was a spectrophotometric quartz cell of 1 cm path length. The photonic flux at 365 nm, measured by ferrioxalate actinometry [74] was equal to 7.40×10^{15} photons s^{-1} cm^{-2}.

Irradiation with Suntest CPS photoreactor (Atlas) was used to simulate the effect of solar light. This is equipped with a Xe lamp (I = 750 W m^{-2}) and filters that prevent the transmission of wavelengths below 290 nm. The temperature was maintained constant at 20 ºC by the water flow from a thermostat bath.

For the determination of the initial rate constants, half-lives and evolution of photoproducts, irradiations of NAD at 365 nm in absence/presence of $W_{10}O_{32}^{4-}$ were carried out in an elliptical stainless steel cylinder under constant stirring. Three high pressure mercury lamps (black lamp, Mazda MAW 125 W) were installed symmetrically in the lower part of the cylinder. Although these emitted mainly at 365 nm (97% of the emission), two incompletely filtered rays at 313 (2.0%) and 334 nm (1.0%) were also present. The reactor, a water-jacketed Pyrex tube ($\phi = 2.8$ cm) containing 50 mL solution and located in the centre of the system, was cooled by the water flow from a thermostat bath (T = 20 °C) during irradiation experiments. To obtain further information on the reactive species involved in NAD degradation pathway, an aerated aqueous mixture of [NAD+$W_{10}O_{32}^{4-}$ (3.0×10^{-4} mol L^{-1})] containing an excess of *iso*-propanol (1.0 mol L^{-1}), known to be hydrogen atom donor [45, 50], was irradiated at 365 nm using the previously described system.

2.3. Analysis

UV/vis absorption spectra were recorded on a Cary 3 double beam spectrophotometer using a 1 cm path length quartz cell. pH measurements were made with a JENWAY 3310 pH-meter to ± 0.01 pH unit. Attenuated Total Reflectance (ATR) Fourier Transform Infrared (FTIR) spectrum was measured in the range 500-4000 cm^{-1} (resolution of 2 cm^{-1} with 15 scans) on a FTIR Nicolet 5700 spectrometer (Thermo Electron Corporation) equipped with a Smart Orbit accessory.

The disappearance of NAD and the formation of photoproducts were monitored by high performance liquid chromatography (HPLC), using a system equipped with a Waters 996 diode array detector (DAD), two Waters 510 pumps and an automatic injector (Waters 717). The wavelength of detection was set at 280 nm. A reverse phase Nucleodur column was used (Eclipse XDB-C18, 5 μm, 250 mm×4.6 mm) with 50% water (pH 3.5

with formic acid) and 50% methanol as eluent. The injected volume was 25 μL and the flow rate 1 mL min^{-1}. Each sample was analyzed by HPLC in triplicate, with a maximum error of 3.0%.

The photoproduct identification was carried out at Université Blaise Pascal using a Waters liquid chromatography (LC) system (Alliance 2695) coupled to a quadrupole time-of-flight mass spectrometer (Micromass) equipped with a pneumatically assisted electro-spray ionization source (ESI). The LC system was also coupled with a Waters 996 diode array detector. Data acquisition and processing were performed by MassLynx NT 3.5 software. Chromatographic separation was achieved by using 50% water (pH 3.5 with formic acid) and 50% methanol as elution program in a Phenomenex column (Kinetex MS C18, 3.5 μm, 100 mm×2.1 mm). The flow rate was set at 0.2 mL min^{-1} and the injected volume was 3.0 μL. The electro-spray source parameters were in positive mode: capillary voltage 3000 V (2100 V in negative mode), cone voltage 35 V, extraction cone voltage 2 V, desolvation temperature 250 °C, source temperature 100 °C, ion energy 2 V and collision energy (CE) between 10 to 30 eV (7 eV in negative mode).

Ionic liquid chromatography was used to measure the evolution in concentration of nitrate, nitrate and ammonia ions as a function of irradiation time, upon mineralization of NAD in presence of $W_{10}O_{32}^{4-}$. For the anions, a Dionex DX320 system with AS11 column was used, while for ammonia a Dionex ICS1500 system with CS16 column was employed, with 1.0 mL min^{-1} flow.

The mineralization of NAD was monitored by measuring the total organic carbon concentration (TOC) with a Shimadzu Model TOC-5050A equipped with an automatic sample injector. The calibration curve was obtained within the range 0-49 mg L^{-1} by using potassium hydrogen phthalate and sodium hydrogen carbonate for organic and inorganic carbon, respectively. Three injections were made for each sample with an error of roughly 5.0%.

3. Results and discussion

3.1. Synthesis and characterization of the catalyst sodium decatungstate

The catalyst sodium decatungstate, $Na_4W_{10}O_{32}.7H_2O$, (designated in its anionic form as decatungstate anion or $W_{10}O_{32}^{4-}$) was synthesized according to a literature procedure [73], and characterized by UV-Vis and infrared spectroscopies. Fig. 1 presents the UV absorption spectrum of an aqueous solution of $W_{10}O_{32}^{4-}$ (3.0×10^{-4} mol L^{-1}) at its natural pH (around 5.0).

The UV spectrum of $W_{10}O_{32}^{4-}$ presents two absorption bands with maxima at 267 and 323 nm, in agreement with the literature [56, 58, 68]. The first band is attributed to $H_2W_{12}O_{40}^{6-}$ and the band at 323 nm corresponds to $W_{10}O_{32}^{4-}$ [68]. Since the metal ions in the fully oxidized POMs have a d^0 electronic configuration, the only absorption band that occurs in the UV range of the electronic spectra is due to the oxygen-to-metal (O→M) charge transfer (LMCT) process [47, 60, 61, 75, 76]. The Fourier Transform Infrared (FTIR) spectrum of $W_{10}O_{32}^{4-}$ (Fig. S1 (support information)) exhibits several vibrational bands with varying intensities that are in perfect agreement with literature data [73].

3.2. Photodegradation of NAD in presence and absence of $W_{10}O_{32}^{4-}$ under simulated solar light irradiation

As illustrated in Fig. 1, the UV absorption spectrum of NAD (3.0×10^{-4} mol L^{-1}) in aqueous solution presents a broad band with vibrational structure extending from 250 to 320 nm, with maximum centred at 280 nm ($\varepsilon_{280\ nm}$ = 6540 L mol^{-1} cm^{-1}, [77]). Despite the small overlap of this absorption band with the emission spectrum of solar light (Fig. 1), NAD is susceptible to degrade under environmental conditions. Therefore, simulated solar light was used as light source (Suntest system) for the irradiation of an aqueous NAD solution (3.0×10^{-4} mol L^{-1}). Its transformation kinetics (Fig. 2) shows that NAD is effectively degraded under these conditions: 51% of disappearance in 8 h. The main products formed under these conditions have already been reported in our previous work [14] and will be referred ahead in the text. However, as also observed in Fig. 1, $W_{10}O_{32}^{4-}$ presents an important overlap (much greater than NAD) with the emission spectrum of solar light within the range 290-400 nm, and this allows it to be used as a photocatalyst for water decontamination. Hence, the effect of the catalyst $W_{10}O_{32}^{4-}$ (3.0×10^{-4} mol L^{-1}) on NAD degradation in aqueous solution was assessed using the Suntest system. The results, given in Fig. 2, provide evidence of the photocatalytic activity of $W_{10}O_{32}^{4-}$ in NAD degradation: 89% disappearance is seen after 8 h of irradiation. These results are in agreement with literature studies regarding the effectiveness of $W_{10}O_{32}^{4-}$ as a catalyst for the degradation of organic pollutants under solar irradiation [34, 56, 58, 70]. Nevertheless, in this situation, both direct and induced phototransformation may contribute to NAD degradation since NAD and $W_{10}O_{32}^{4-}$ both absorb at $\lambda > 290$ nm. Consequently, and since the main goal of this work was to study the degradation of NAD promoted by the catalyst $W_{10}O_{32}^{4-}$, further studies were performed using a powerful and selective irradiation system at 365 nm. Under these conditions, the direct photolysis of

NAD is absent, and only $W_{10}O_{32}^{4-}$ will be responsible for NAD disappearance. This allows assessment of the efficiency of the catalyst on the degradation process.

3.3. Direct degradation of NAD under irradiation at 365 nm

The direct irradiation of aerated aqueous NAD solutions (3.0×10^{-4} mol L^{-1}) was first evaluated in the absence of $W_{10}O_{32}^{4-}$ with the 365 nm light source. This test will help us to assess the catalytic efficiency of $W_{10}O_{32}^{4-}$ towards NAD degradation. Under these conditions (Fig. 3), good stability of the pesticide is observed after 22 h of irradiation (5.0% of degradation) and no formation of products was observed. Since NAD does not absorb at 365 nm, the small disappearance observed can be explained by the presence of the incompletely filtered rays at 313 nm present in the 365 nm irradiation system.

3.4. Photocatalytic degradation of NAD in the presence of $W_{10}O_{32}^{4-}$ at 365 nm
3.4.1. Effect of oxygen concentration

The photocatalytic degradation of aqueous NAD solutions (3.0×10^{-4} mol L^{-1}) in the presence of $W_{10}O_{32}^{4-}$ (3.0×10^{-4} mol L^{-1}) under illumination at 365 nm was studied as a function of oxygen concentration: aerated, de-aerated and oxygen saturated conditions. The kinetic results are depicted in Fig. 3, while the initial rate constants, half-lives and quantum yields of NAD transformation in the presence of $W_{10}O_{32}^{4-}$ are reported in Table 1. The kinetic profile presented in Fig. 3 provides evidence for the significant role that oxygen plays in the NAD photocatalysed degradation. The degradation rate follows the order: aerated $\cong$ oxygenated > de-aerated.

Under aerated conditions, 95% of the NAD disappeared after 22 h of irradiation, with an estimated first-order rate constant of 3.2×10^{-3} min^{-1}. This indicates that the catalyst $W_{10}O_{32}^{4-}$ enhanced NAD degradation by a factor of 19 when compared with direct NAD degradation (k $\cong 1.5\times10^{-4}$ min^{-1}). Furthermore, the addition of oxygen to the solution did not significantly increase the photocatalytic activity of $W_{10}O_{32}^{4-}$, as can be seen in Fig. 3. In fact, the quantum yields, half-lives and rate constants given in Table 1 indicate that degradation is of the same order of magnitude in aerated conditions when compared with oxygenated conditions. Such a result indicates that the oxygen concentration existing in solution was sufficient for the regeneration of the initial form $W_{10}O_{32}^{4-}$, leading to the continuous degradation of NAD through the photocatalytic cycle. The presence of oxygen is vital to reoxidize the reduced form $W_{10}O_{32}^{5-}$ to its initial form

$W_{10}O_{32}^{4-}$, closing the photocatalytic cycle [56, 69], but is not involved in the initial photochemical step. The oxygen consumption in the reoxidation step with reduced tungstate probably leads to the formation of superoxide anion, which can further participate in the degradation process leading, on protonation, to hydroperoxyl species [56]. However, no further studies were done to detect these species.
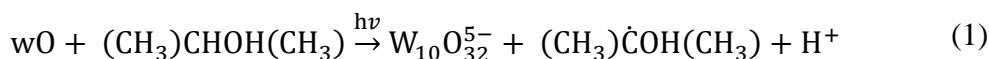
Under de-aerated conditions, at the earliest times of irradiation, a slight degradation of NAD was observed (Fig. 3), after which it was almost completely inhibited (94% after 22 h). This small decrease may be due to the direct degradation of NAD but also to the presence of some residual oxygen left in solution, and $W_{10}O_{32}^{4-}$ availability present in initial times. The involvement of residual oxygen and initial $W_{10}O_{32}^{4-}$ in this step is clearly demonstrated by the quantum yield determined under these conditions using monochromatic irradiation at 365 nm (Table 1). After this, a plateau was reached, owing to the formation of decatungstate excited species, wO [60-64], that decays to form the one electron reduced species $W_{10}O_{32}^{5-}$. This accumulates in the course of the reaction since there is no more oxygen to oxidize it back to the initial $W_{10}O_{32}^{4-}$, leading to the breaking of the catalytic cycle. Moreover, the formation of a blue color was observed after the earliest times of irradiation, and persisted till the end of the irradiation, which is consistent with the formation of the reduced species $W_{10}O_{32}^{5-}$, that presents an absorption maximum at 780 nm [76]. When this solution was left exposed to air, the blue color disappeared, confirming that oxygen plays an important role on regenerating the reduced species $W_{10}O_{32}^{5-}$ to the starting form of the catalyst, $W_{10}O_{32}^{4-}$.

The irradiation of aerated and oxygenated NAD aqueous solutions in presence of $W_{10}O_{32}^{4-}$ at 365 nm revealed the formation of several photoproducts, as will be discussed ahead in text. On the other hand, no products were observed in de-aerated conditions or even when NAD photolysis was performed at 365 nm in absence of $W_{10}O_{32}^{4-}$ (see section 3.3).

3.4.2. Effect of *iso*-propanol

The kinetic profile of the aqueous aerated mixture [NAD+$W_{10}O_{32}^{4-}$ (3.0×10^{-4} mol L^{-1})] irradiated at 365 nm in the presence of an excess of *iso*-propanol (1.0 mol L^{-1}) is depicted in Fig. 3. Under these conditions, 11% of NAD disappeared in the first 60 min of irradiation, after which, complete inhibition of degradation was observed until 22 h of irradiation. This initial decrease of NAD concentration was accompanied by the

formation of the blue color, typical of the one electron reduced species $W_{10}O_{32}{}^{5-}$, whose yield is known to increase in presence of *iso*-propanol [45]. Within the first 60 min, NAD disappearance may be explained by the competition between *iso*-propanol and the available $W_{10}O_{32}{}^{4-}$ to form the reactive species wO responsible for NAD transformation. After this time, the inhibition of NAD degradation in the presence of *iso*-propanol may be explained by the efficient trapping of the reactive excited species wO by the alcohol. This suggests the involvement of hydrogen atom abstraction (HA) by the excited state of $W_{10}O_{32}{}^{4-}$, wO, from *iso*-propanol [50], leading to the formation and accumulation of the reduced form $W_{10}O_{32}{}^{5-}$, as shown by the blue coloration. The classical reaction of the excited species wO with *iso*-propanol via HA is proposed in reactions (1) to (4):
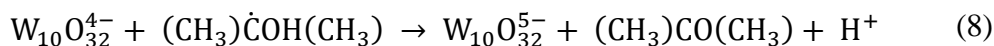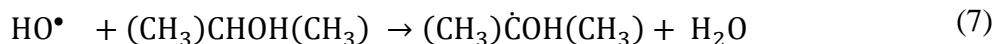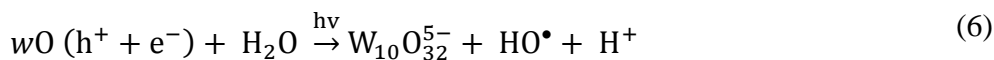
$$wO + (CH_3)CHOH(CH_3) \xrightarrow{h\nu} W_{10}O_{32}^{5-} + (CH_3)\dot{C}OH(CH_3) + H^+ \quad\quad (1)$$

$$(CH_3)\dot{C}OH(CH_3) + O_2 \rightarrow (CH_3)CO(CH_3) + HO_2^{\bullet} \quad\quad (2)$$

$$W_{10}O_{32}^{5-} + O_2 + H^+ \rightarrow W_{10}O_{32}^{4-} + HO_2^{\bullet} \quad\quad (3)$$

$$2HO_2^{\bullet} \rightarrow H_2O_2 + O_2 \quad\quad (4)$$

The overall photocatalytic oxidation of *iso*-propanol in the presence of oxygen and $W_{10}O_{32}{}^{4-}$ is given by reaction (5), in which the alcohol is transformed into acetone and hydrogen peroxide:

$$(CH_3)CHOH(CH_3) + O_2 + W_{10}O_{32}^{4-} \xrightarrow{hv} (CH_3)CO(CH_3) + H_2O_2 \quad\quad (5)$$
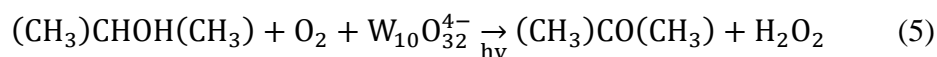
The results obtained with *iso*-propanol are in agreement with literature mechanistic studies, which show that in photosensitized oxidations of organic substrates by $W_{10}O_{32}{}^{4-}$ in the presence of oxygen, either HA or electron transfer (ET) or even both mechanisms may occur [67, 79-81]. We note, however, that some authors suggest that the reactive species wO also reacts with organic substrates in aqueous solution by indirect H abstraction via hydroxyl radicals. These radicals may be formed through the reaction of wO with water molecules (oxidative trapping holes) [65, 71] since the excited state potential of the decatungstate is more positive than the one-electron oxidation of water [71] (reaction 6). The HO$^{\bullet}$ radicals thus formed react with organic substrates mainly via α-C H abstraction (reaction 7). The highly reducing hydroxyl alkyl radical formed $(CH_3)C^{\bullet}OH(CH_3)$ reacts further with the polyoxometalate (reaction 8). In the absence of strong oxidant agents (such as oxygen), electrons accumulate on the polyoxometalate,

driving the redox potential to more negative values until an oxidant in solution is able to act as electron acceptor and close the photocatalytic cycle.

$$wO\ (h^+ + e^-) + H_2O \xrightarrow{h\nu} W_{10}O_{32}^{5-} + HO^\bullet + H^+ \tag{6}$$

$$HO^\bullet + (CH_3)CHOH(CH_3) \rightarrow (CH_3)\dot{C}OH(CH_3) + H_2O \tag{7}$$

$$W_{10}O_{32}^{4-} + (CH_3)\dot{C}OH(CH_3) \rightarrow W_{10}O_{32}^{5-} + (CH_3)CO(CH_3) + H^+ \tag{8}$$

However, even though there are some experimental results in the literature that appear to support the formation of HO$^\bullet$ radicals in these systems, this possibility is still a matter of debate and no consensus exists on it.

3.5. Mineralization process

The mineralization of NAD aqueous aerated solution (3.0×10^{-4} mol L^{-1}) in the presence of $W_{10}O_{32}^{4-}$ (3.0×10^{-4} mol L^{-1}) was followed by TOC measurement as a function of irradiation time using 365 nm light (Fig. 4). Under our experimental conditions, $W_{10}O_{32}^{4-}$ efficiently promotes NAD mineralization: 73% was achieved after 500 h of irradiation. However, from Figs. 2 and 4, it can be seen that the degradation of NAD in the presence of $W_{10}O_{32}^{4-}$ takes place much faster than mineralization. Almost 100% of NAD degradation is achieved after 22 h of irradiation, while more than 500 h are necessary for complete mineralization. This is probably related with the formation of huge amounts of intermediate species formed during the course of NAD photodegradation, that require longer time to be further oxidised, leading therefore to mineralization on a longer time scale.

The formation of the inorganic anions (nitrates, nitrites) and ammonium ions following photolysis in the presence of $W_{10}O_{32}^{4-}$ was also evaluated under the same experimental conditions. The concentration of NO$_2^-$ during the course of reaction presents values at trace levels, < 6.0 μg L^{-1} and NH$_4^+$ presents concentrations < 0.5 mg L^{-1}. NO$_3^-$, on the other hand, has a more important contribution, and a correlation can be made between the decrease of TOC and the formation of NO$_3^-$, as shown in Fig. 4. After 500 h of irradiation, 73% of NAD is mineralized and the concentration of NO$_3^-$ is equal to 2.6 mg L^{-1}, very close, within the experimental errors, to the expected value calculated from the NAD concentration (2.7 mg L^{-1}). These results confirm the mineralization of NAD on photolysis in the presence of $W_{10}O_{32}^{4-}$.

3.6. Identification of NAD degradation products in the presence of $W_{10}O_{32}^{4-}$

Solutions of NAD irradiated at 365 nm in the presence of $W_{10}O_{32}^{4-}$ were analysed by HPLC-DAD and by LC-MS. Since many products were formed under these conditions, aerated and oxygenated solutions of (NAD+$W_{10}O_{32}^{4-}$) irradiated at certain times of conversion (10, 30 and 50%) were further analysed by LC-MS/MS with electron spray ionisation (ES) in positive (ES$^+$) as well as negative mode (ES$^-$) to identify the main photoproducts. Although both ionization modes were employed, the best response was obtained with ES$^+$, as shown in the chromatogram presented in Fig. 5. Several products are formed and almost all present shorter retention times than NAD (10.8 min), indicating the formation of more polar photoproducts. The exception was the product eluted at 11.3 min which corresponds to 1-naphthylacetic acid (1-NAA), in agreement with a previous study that reports this as NAD degradation product [12]. Based on these results, thirteen main products were identified by the molecular ion ([M+H]$^+$ and [M-H]$^-$) and their mass fragments ions (Table 2).

3.6.1. Characterization of the parent compound NAD

The NAD mass spectrum and the fragmentation pattern obtained by LC-MS/MS (ES$^+$ mode) is given in Fig. S2 and Scheme S1 (support information), respectively. In addition to the molecular ion of NAD [M+H]$^+$ with $m/z = 186$, a main fragment ion was observed at $m/z = 141$. This corresponds to the loss of the amide group [M+H-CONH$_3$]$^+$ and is in agreement with literature data [82, 83]. Another fragment ion with $m/z = 169$ was observed in the mass spectrum, although with a low abundance. This ion corresponds to the loss of ammonia [M+H-NH$_3$]$^+$. Further fragmentation of the molecular ion at 186 yields the ion with $m/z = 115$ with higher collision energy (CE), as depicted in the inset of Fig. S2, which may be explained by the loss of an olefin group [M+H-CONH$_3$-C$_2$H$_2$]$^+$.

3.6.2. Characterization of the product 1-naphthylacetic acid

The only product with retention time greater than NAD (11.3 min) corresponds to the compound 1-naphthylacetic acid (1-NAA). The amide group of NAD is hydrolysed to yield the respective acid 1-NAA and NH$_3$ (and NH$_4^+$) (Scheme 1). Since 1-NAA is commercially available, its identification was made by comparing the obtained retention

time and the UV-vis absorption spectrum ($\lambda_{max} \cong 280$ nm) of a sample injected in LC-DAD using the same conditions as NAD.

3.6.3. Characterization of hydroxylated products

Firstly, the presence of hydroxylated NAD derivatives was assumed regarding mass differences between by-products and NAD of 16, 32 and 48 mDa. Furthermore, fragmentation of by-products helps confirming their formation.

In fact, products with retention times of 9.4 and 10.3 min were detected from the early stages of the irradiation. These products, both having m/z ratio 202 ($[M+H]^+$), but different fragmentation patterns, were attributed to mono-hydroxylated forms of NAD (Table 2). The hydroxylation of the aromatic ring to give the mono-substituted products can occur at either of the two aromatic rings of NAD. Taking into account the fragmentation results, the product at 10.3 min presents as main fragment ions $m/z = 185$, 157 and 143, corresponding to the loss of NH_3^+, acetamide ($CO\text{-}NH_3^+$) and $CH_2\text{-}CO\text{-}NH_3^+$ groups, respectively, thus confirming the assignment. The other product observed at 9.4 min presents as main fragment ions $m/z = 184$ and 156 that indicate the loss of a water molecule and of $CO\text{-}H_2O$, respectively, is also in agreement with hypothesis.

Several photoproducts with molecular ion peak at $m/z = 218$ ($[M+H]^+$) were detected with retention times 6.6, 7.4, 7.8, 8.2, 8.6 and 9.0 min. Fig. 6 shows, as example, the MS^2 spectrum of $m/z = 218$ for the compound eluted at 8.2 min. The diverse fragments suggest the formation of various isomers of di-hydroxylated products, either involving one or both aromatic rings (Table 2). Fragmentation of isomers leads to the loss of one or two water molecules, amino group, amido side-chain and combination that confirm the structure of di-hydroxylated products.

Two products with molecular ion peak $m/z = 234$ ($[M+H]^+$) and retention times of 6.0 and 7.1 min have been detected. Main fragments of the products correspond to the loss of one or two H_2O molecule, together with the loss of carbonyl function and amido side chain. The presence of these fragments is in good accordance with tri-hydroxylated derivatives of NAD (Table 2).

Such hydroxylated compounds (mono and dihydroxylated) are among the major products found in photodegradation studies of naphthalene and naphthalene derivatives in solution, either under direct or sensitized degradation [84-88] [89]. Although several authors have proposed the formation of the tri-hydroxy compounds in the mechanism of

naphthalene degradation [89], they have not been clearly identified in these studies, but results are in accordance with our assignment.

3.6.4. Characterization of the naphthoquinone and derivative products

A photoproduct with retention time of 8.8 min was assigned to the naphthoquinone formed from NAD. The molecular ion with $m/z = 216$ ([M+H]$^+$) presents fragments at 199, 171 and 143. These indicate the loss of NH_3, CO-NH_3^+ and also CO-CO-NH_3 groups, respectively, which is in agreement with the proposed naphthoquinone compound. Furthermore, these results were also corroborated by the LC-ESI-MS analysis in negative mode ($m/z = 214$ for [M-H]$^-$). Although two possible isomers may be attributed to this compound, the most stable structure corresponds to the one having the carbonyl groups in the 1,4-position of the free aromatic ring (Table 2) since the 1,2-naphthoquinone will be unstable, and likely to lead to the opening of the ring. Two products with a molecular ion peak [M+H]$^+$ with $m/z = 232$ and retention times of 6.8 and 9.5 min were detected, and identified as the hydroxy-naphthoquinone derivatives (Table 2). The main fragments of the product at 6.8 min have a ratio $m/z = 214$, 200, 172 and 155. These are attributed to the loss of H_2O molecule, H_2O-CH_2, H_2O-CH_2-CO and H_2O-CH_2-CO-NH_3^+. The product eluted at 9.5 min has as fragmentation pattern 216, 200, 172 and 155 (Fig. 7). These correspond to the loss of one (216) and two oxygen atoms (200), O_2-CO and O_2-$CONH_3^+$, respectively. Naphthoquinones and hydroxyl-naphthoquinone derivatives have been reported in the literature as naphthalene oxidative degradation products [87, 88, 90].

3.7. Proposed mechanistic pathways

Based on the above results, a mechanism of the primary steps of NAD photocatalysed degradation by $W_{10}O_{32}{}^{4-}$ involving electron transfer and HA abstraction is proposed in Scheme 2. The absorption of light by $W_{10}O_{32}{}^{4-}$ in its ground state leads to the formation of an oxygen-to-metal charge transfer excited state $W_{10}O_{32}{}^{4-*}$ [61] that decays in few picoseconds in both aerated and de-aerated solutions to form the very reactive non-emissive transient species wO [61, 91]. According to the photoproducts identified by LC-ESI-MS, the first step of the photodegradation should correspond to an electron transfer process involving the reactive species wO and the aromatic ring of NAD, with consequent formation of NAD$^{\bullet+}$ radical cation and the reduced decatungstate species, $W_{10}O_{32}{}^{5-}$ [76, 92]. The reaction of NAD$^{\bullet+}$ radical cation with water leads to the

hydroxylation of the aromatic ring. Two mono-hydroxylated products were identified as primary products. Such hydroxylated products have previously been seen in naphthalene and naphthalene derivative photodegradation [84-88]. Subsequent reaction of the mono-hydroxylated products with oxygen leads to the formation of the di- and tri-hydroxylated NAD products. The proposed naphthoquinone derivative may arise from two different pathways. One involves hydrogen abstraction (HA) of the di-hydroxylated NAD product (step b). Since the exact positions of the OH groups on the aromatic ring are not known, the structures drawn correspond to the most stable one in 1,4-position. Another possibility starts with the deprotonation of the NAD radical formed, followed by an oxygenation process, leading to the formation of an unstable endoperoxide at positions 1,4-, which dissociates in the presence of light into the 1,4-naphthoquinone derivative (step a). The hydroxylation of this naphthoquinone derivative leads to the hydroxyl-1,4-naphthoquinone. The hydroxyl-1,4-naphthoquinone derivative would be expected to have greater stability than the parent 1,2-naphthoquinone as the hydroxyl group would stabilize the quinone due to hydrogen bonding between the hydroxyl group and the oxygen on carbon 1. For prolonged photolysis times, it is expected that the irradiation of the tri-hydroxylated products leads to the opening of the aromatic ring, with formation of various aliphatic derivatives, which, in turn, can undergo oxidation and decarboxylation steps with the formation of CO_2 as final product. The opening of the ring has been reported in several studies concerning the degradation of naphthalene and its derivatives, either by direct or photocatalysed degradation [86, 87, 89, 90]. In the presence of oxygen, $W_{10}O_{32}^{5-}$ is oxidized to its initial form, $W_{10}O_{32}^{4-}$, closing the catalytic cycle (Scheme 2). The oxygen consumption is accompanied by its reductive activation to form the superoxide anion, which ultimately leads to the formation of peroxy products.

A comparison between the products of NAD degradation under direct excitation previously studied [14], and those identified in this work (photocatalysed excitation by $W_{10}O_{32}^{4-}$) reveals some similarities, but also some differences, suggesting differences in the mechanisms of degradation. The hydroxylated (mono- and di-) as well as the naphthoquinone products were identified in both situations, whereas the furanone and coumarin compounds were only found under NAD direct irradiation [14]. In contrast, tri-hydroxylation and hydroxyl-naphthoquinone products were only identified in the photocatalysed degradation of NAD in the presence of $W_{10}O_{32}^{4-}$. The formation of these tri-hydroxylated products may be favoured by the proximity of the catalyst, which

ultimately will lead to the ring opening and to the mineralization process, which does not occur under direct degradation.

4. Conclusions

The use of the catalyst decatungstate anion ($W_{10}O_{32}^{4-}$) in the homogenous degradation of NAD in water under UV and simulated solar light exposure has proved to be very efficient. The effect of oxygen concentration on this photocatalysed degradation indicates a faster degradation of NAD under aerated conditions. This indicates the important role of oxygen in the regeneration of the catalyst to favor the photocatalytic cycle. In addition, mineralization studies show that NAD is, indeed, converted into CO_2, H_2O and nitrates as main inorganic products. The identification of NAD primary products was also assessed, and from this a degradation mechanistic scheme was proposed. The primary steps of NAD degradation involve electron transfer as well as hydrogen atom abstraction processes. Electron transfer occurs between the aromatic ring of NAD and the reactive species of excited decatungstate, with consequent formation of $NAD^{\bullet+}$ radical cation and the reduced decatungstate species. As a consequence, hydroxylation and oxidation products were identified and no reactivity of NAD amide side chain was observed. Similarly, new NAD photoproducts were formed and identified in the presence of the catalyst when compared with direct photolysis.

References

[1] M. Biziuk, A. Przyjazny, J. Czerwinski, M. Wiergowski, Occurrence and determination of pesticides in natural and treated waters, J. Chrom. A 754 (1996) 103-123.

[2] S. Stehle, R. Schulz, Agricultural insecticides threaten surface waters at the global scale, Proc. Natl. Acad. Sci. U. S. A. 112 (2015) 5750-5755.

[3] R. Grover, A.J. Cessna, Environmental Chemistry of Herbicides, CRC Press, Taylor & Francis Group, Boca Raton, Florida, 1991.

[4] P.V.L. Reddy, K.-H. Kim, A review of photochemical approaches for the treatment of a wide range of pesticides, J. Hazard. Mat. 285 (2015) 325-335.

[5] A. Blair, M. Dosemeci, E.F. Heineman, Cancer and other causes of death among male and female farmers from twenty-three states, Am. J. Ind. Med. 23 (1993) 729-742.

[6] L. Yáñez, D. Ortiz, J. Calderón, L. Batres, L. Carrizales, J. Mejía, L. Martínez, E. García-Nieto, F. Díaz-Barriga, Overview of human health and chemical mixtures: problems facing developing countries, Environ. Health Perspect. 110 (2002) 901-909.

[7] WHO, Public health impact of pesticides used in agriculture, in, WHO (World Health Organization), Geneva, 1990.

[8] UNEP, Childhood pesticide poisoning: information for advocacy and action, in, United Nations Environment Programme (UNEP), Switzerland, 2004, 37.

[9] C. Infante-Rivard, S. Weichenthal, Pesticides and childhood cancer: an update of Zahm and Ward's 1998 review, J. Toxicol. Environ. Health B Crit. Rev. 10 (2007) 81-99.

[10] EPA, Registration eligibility decision (RED) for naphthaleneacetic acid, its salts, ester and acetamide, in, USA Environmental Protection Agency (US EPA), United States of America, 2007.

[11] C.D.S. Tomlin, The Pesticide Manual, Twelfth edition ed., British Crop Protection Council, UK, 2000.

[12] EFSA, Conclusion on the peer review of the pesticide risk assessment of the active substance 2-(1-naphthyl)acetamide (notified as 1-naphthylacetamide), EFSA (European Food Safety Authority) Journal, 9(2):2020 (2011) 58.

[13] F.E. Gardner, Practical applications of plant growth substances in horticulture, P. Fl. St. Hortic. Soc. 54 (1941) 20-26.

[14] E.S. Da Silva, P. Wong-Wah-Chung, H.D. Burrows, M. Sarakha, Photochemical degradation of the plant growth regulator 2-(1-naphthyl) acetamide in aqueous solution upon UV irradiation, Photochem. Photobiol. 89 (2013) 560-570.

[15] R. Andreozzi, V. Caprio, A. Insola, R. Marotta, Advanced oxidation processes (AOP) for water purification and recovery, Catal. Today, 53 (1999) 51-59.

[16] S. Chiron, A. Fernandez-Alba, A. Rodriguez, E. Garcia-Calvo, Pesticide chemical oxidation: state-of-the-art, Water Res. 34 (2000) 366-377.

[17] C. Comninellis, A. Kapalka, S. Malato, S.A. Parsons, I. Poulios, D. Mantzavinos, Advanced oxidation processes for water treatment: advances and trends for R&D, J. Chem. Technol. Biotechnol. 83 (2008) 769-776.

[18] R. Homlok, E. Takács, L. Wojnárovits, Degradation of organic molecules in advanced oxidation processes: Relation between chemical structure and degradability, Chemosphere, 91 (2013) 383-389.

[19] O. Legrini, E. Oliveros, A.M. Braun, Photochemical processes for water treatment, Chem. Rev. 93 (1993) 671-698.

[20] M.A. Oturan, J.-J. Aaron, Advanced Oxidation Processes in Water/Wastewater Treatment: Principles and Applications. A Review, Crit. Rev. Env. Sci. Tec. 44 (2014) 2577-2641.

[21] W.H. Glaze, J.-W. Kang, D.H. Chapin, The Chemistry of Water Treatment Processes Involving Ozone, Hydrogen Peroxide and Ultraviolet Radiation, Ozone-Sci. Eng. 9 (1987) 335-352.

[22] K. Ikehata, M. Gamal El-Din, Aqueous Pesticide Degradation by Ozonation and Ozone-Based Advanced Oxidation Processes: A Review (Part II), Ozone-Sci. Eng. 27 (2005) 173-202.

[23] M. Tamimi, S. Qourzal, N. Barka, A. Assabbane, Y. Ait-Ichou, Methomyl degradation in aqueous solutions by Fenton's reagent and the photo-Fenton system, Sep. Purif. Technol. 61 (2008) 103-108.

[24] M.N. Chong, B. Jin, C.W.K. Chow, C. Saint, Recent developments in photocatalytic water treatment technology: A review, Water Res. 44 (2010) 2997-3027.

[25] S. Devipriya, S. Yesodharan, Photocatalytic degradation of pesticide contaminants in water, Sol. Energ. Mat. Sol. Cells 86 (2005) 309-348.

[26] J.-M. Herrmann, Heterogeneous photocatalysis: fundamentals and applications to the removal of various types of aqueous pollutants, Catal. Today 53 (1999) 115-129.

[27] M.R. Hoffmann, S.T. Martin, W. Choi, D.W. Bahnemann, Environmental Applications of Semiconductor Photocatalysis, Chem. Rev. 95 (1995) 69-96.

[28] S. Malato, J. Blanco, J. Cáceres, A.R. Fernández-Alba, A. Agüera, A. Rodríguez, Photocatalytic treatment of water-soluble pesticides by photo-Fenton and TiO_2 using solar energy, Catal. Today 76 (2002) 209-220.

[29] U.I. Gaya, A.H. Abdullah, Heterogeneous photocatalytic degradation of organic contaminants over titanium dioxide: A review of fundamentals, progress and problems, J. Photochem. Photobiol. C: Photochem. Rev. 9 (2008) 1-12.

[30] I.K. Konstantinou, T.A. Albanis, Photocatalytic transformation of pesticides in aqueous titanium dioxide suspensions using artificial and solar light: intermediates and degradation pathways, Appl. Catal., B 42 (2003) 319-335.

[31] A.L. Linsebigler, G. Lu, J.T. Yates, Photocatalysis on TiO_2 Surfaces: Principles, Mechanisms, and Selected Results, Chem. Rev. 95 (1995) 735-758.

[32] M. Pelaez, N.T. Nolan, S.C. Pillai, M.K. Seery, P. Falaras, A.G. Kontos, P.S.M. Dunlop, J.W.J. Hamilton, J.A. Byrne, K. O'Shea, M.H. Entezari, D.D. Dionysiou, A review on the visible light active titanium dioxide photocatalysts for environmental applications, Appl. Catal., B 125 (2012) 331-349.

[33] E. Gkika, P. Kormali, S. Antonaraki, D. Dimoticali, E. Papaconstantinou, A. Hiskia, Polyoxometallates as effective photocatalysts in water purification from pesticides, Int. J. Photoenergy 6 (2004) 227-231.

[34] A. Mylonas, A. Hiskia, E. Papaconstantinou, Contribution to water purification using polyoxometalates. Aromatic derivatives, chloroacetic acids, J. Mol. Catal. A: Chem. 114 (1996) 191-200.

[35] A. Mylonas, E. Papaconstantinou, On the mechanism of photocatalytic degradation of chlorinated phenols to CO_2 and HCl by polyoxometalates, J. Photochem. Photobiol. A: Chem. 94 (1996) 77-82.

[36] A. Hiskia, A. Troupis, E. Papaconstantinou, Environmental photocatalytic processes with POM. The photodecomposition of atrazine and photoreduction of metal ions from aqueous solutions, Int. J. Photoenergy 4 (2002) 35-40.

[37] A. Hiskia, E. Androulaki, A. Mylonas, A. Troupis, E. Papaconstantinou, Photocatalytic Decontamination by Polyoxometalates, in: M.T. Pope, A. Müller (Eds.) Polyoxometalate Chemistry From Topology via Self-Assembly to Applications, Springer Netherlands, Dordrecht, 2001, 417-424.

[38] A. Hiskia, E. Androulaki, A. Mylonas, S. Boyatzis, D. Dimoticali, C. Minero, E. Pelizzetti, E. Papaconstantinou, Photocatalytic mineralization of chlorinated organic pollutants in water by polyoxometallates. Determination of intermediates and final degradation products, Res. Chem. Intermed. 26 (2000) 235-251.

[39] A. Hiskia, M. Ecke, A. Troupis, A. Kokorakis, H. Hennig, E. Papaconstantinou, Sonolytic, Photolytic, and Photocatalytic Decomposition of Atrazine in the Presence of Polyoxometalates, Environ. Sci. Technol. 35 (2001) 2358-2364.

[40] A. Hiskia, A. Mylonas, E. Papaconstantinou, Comparison of the photoredox properties of polyoxometallates and semiconducting particles, Chem. Soc. Rev. 30 (2001) 62-69.

[41] E. Papaconstantinou, A. Hiskia, Photochemistry and Photocatalysis by Polyoxometalates, in: J.J. Borrás-Almenar, E. Coronado, A. Müller, M. Pope (Eds.) Polyoxometalate Molecular Science, Springer Netherlands, Dordrecht, 2003, 381-416.

[42] I. Texier, J. Ouazzani, J. Delaire, C. Giannotti, Study of the mechanisms of the photodegradation of atrazine in the presence of two photocatalysts: TiO_2 and $Na_4W_{10}O_{32}$, Tetrahedron, 55 (1999) 3401-3412.

[43] P. Kormali, A. Troupis, T. Triantis, A. Hiskia, E. Papaconstantinou, Photocatalysis by polyoxometallates and TiO_2: A comparative study, Catal. Today 124 (2007) 149-155.

[44] M. Pope, Heteropoly and Isopoly Oxometalates, Springer-Verlag Berlin Heidelberg, West Berlin, 1983.

[45] E. Papaconstantinou, Photochemistry of polyoxometallates of molybdenum and tungsten and/or vanadium, Chem. Soc. Rev. 18 (1989) 1-31.

[46] M.T. Pope, A. Müller, Polyoxometalate Chemistry: An Old Field with New Dimensions in Several Disciplines, Angew. Chem. Int. Ed. Engl. 30 (1991) 34-48.

[47] T. Yamase, Photoredox Chemistry of Polyoxometalates as a Photocatalyst, Catal. Surv. Asia 7 (2003) 203-217.

[48] X. Lopez, J.A. Fernandez, J.M. Poblet, Redox properties of polyoxometalates: new insights on the anion charge effect, Dalton Trans. (2006) 1162-1167.

[49] Y.-F. Song, R. Tsunashima, Recent advances on polyoxometalate-based molecular and composite materials, Chem. Soc. Rev. 41 (2012) 7384-7402.

[50] D.E. Katsoulis, A Survey of Applications of Polyoxometalates, Chem. Rev. 98 (1998) 359-388.

[51] D.-L. Long, E. Burkholder, L. Cronin, Polyoxometalate clusters, nanostructures and materials: From self assembly to designer materials and devices, Chem. Soc. Rev. 36 (2007) 105-121.

[52] J.T. Rhule, C.L. Hill, D.A. Judd, R.F. Schinazi, Polyoxometalates in Medicine, Chem. Rev. 98 (1998) 327-358.

[53] T. Yamase, Photo- and Electrochromism of Polyoxometalates and Related Materials, Chem. Rev. 98 (1998) 307-326.

[54] C.L. Hill, C.M. Prosser-McCartha, Homogeneous catalysis by transition metal oxygen anion clusters, Coord. Chem. Rev. 143 (1995) 407-455.

[55] M. Sadakane, E. Steckhan, Electrochemical Properties of Polyoxometalates as Electrocatalysts, Chem. Rev. 98 (1998) 219-238.

[56] C. Tanielian, Decatungstate photocatalysis, Coord. Chem. Rev. 178–180, Part 2 (1998) 1165-1181.

[57] M.D. Tzirakis, I.N. Lykakis, M. Orfanopoulos, Decatungstate as an efficient photocatalyst in organic chemistry, Chem. Soc. Rev. 38 (2009) 2609-2621.

[58] I. Texier, C. Giannotti, S. Malato, C. Richter, J. Delaire, Solar photodegradation of pesticides in water by sodium decatungstate, Catal. Today 54 (1999) 297-307.

[59] I. Texier, C. Giannotti, S. Malato, C. Richter, J. Ouazzani, J.A. Delaire, Potential applications of solar reactions photocatalysed by the decatungstate anion, J. Chim. Phys. Phys.-Chim. Biol. 96 (1999).

[60] D.C. Duncan, T.L. Netzel, C.L. Hill, Early-Time Dynamics and Reactivity of Polyoxometalate Excited States. Identification of a Short-Lived LMCT Excited State and a Reactive Long-Lived Charge-Transfer Intermediate following Picosecond Flash Excitation of $[W_{10}O_{32}]^{4-}$ in Acetonitrile, Inorg. Chem. 34 (1995) 4640-4646.

[61] D.C. Duncan, M.A. Fox, Early Events in Decatungstate Photocatalyzed Oxidations: A Nanosecond Laser Transient Absorbance Reinvestigation, J. Phys. Chem. A 102 (1998) 4559-4567.

[62] C. Tanielian, K. Duffy, A. Jones, Kinetic and Mechanistic Aspects of Photocatalysis by Polyoxotungstates: A Laser Flash Photolysis, Pulse Radiolysis, and Continuous Photolysis Study, J. Phys. Chem. B 101 (1997) 4276-4282.

[63] I. Texier, J.-F. Delouis, J.A. Delaire, C. Giannotti, P. Plaza, M.M. Martin, Dynamics of the first excited state of the decatungstate anion studied by subpicosecond laser spectroscopy, Chem. Phys. Lett. 311 (1999) 139-145.

[64] I. Texier, J.A. Delaire, C. Giannotti, Reactivity of the charge transfer excited state of sodium decatungstate at the nanosecond time scale, Phys. Chem. Chem. Phys. 2 (2000) 1205-1212.

[65] A. Mylonas, A. Hiskia, E. Androulaki, D. Dimotikali, E. Papaconstantinou, New aspect of the mechanism of photocatalytic oxidation of organic compounds by polyoxometalates in aqueous solutions. The selective photooxidation of propan-2-ol to propanone: The role of OH radicals, Phys. Chem. Chem. Phys. 1 (1999) 437-440.

[66] C. Tanielian, C. Schweitzer, R. Seghrouchni, M. Esch, R. Mechin, Polyoxometalate sensitization in mechanistic studies of photochemical reactions: the decatungstate anion as a reference sensitizer for photoinduced free radical oxygenations of organic compounds, Photochem. Photobiol. Sci. 2 (2003) 297-305.

[67] C. Tanielian, R. Seghrouchni, C. Schweitzer, Decatungstate Photocatalyzed Electron-Transfer Reactions of Alkenes. Interception of the Geminate Radical Ion Pair by Oxygen, J. Phys. Chem. A 107 (2003) 1102-1111.

[68] Y. Nosaka, T. Takei, N. Fujii, Photoinduced reduction of $W_{10}O_{32}^{4-}$ by organic compounds in aqueous solution, J. Photochem. Photobiol. A: Chem. 92 (1995) 173-179.

[69] A. Hiskia, E. Papaconstantinou, Photocatalytic oxidation of organic compounds by polyoxometalates of molybdenum and tungsten. Catalyst regeneration by dioxygen, Inorg. Chem. 31 (1992) 163-167.

[70] S. Rafqah, P.W.-W. Chung, C. Forano, M. Sarakha, Photocatalytic degradation of metsulfuron methyl in aqueous solution by decatungstate anions, J. Photochem. Photobiol. A: Chem. 199 (2008) 297-302.

[71] A. Molinari, R. Argazzi, A. Maldotti, Photocatalysis with $Na_4W_{10}O_{32}$ in water system: Formation and reactivity of OH radicals, J. Mol. Catal. A: Chem. 372 (2013) 23-28.

[72] G. Zhang, Y. Xu, Polyoxometalate-mediated reduction of dichromate under UV irradiation, Inorg. Chem. Comm. 8 (2005) 520-523.

[73] R.F. Renneke, M. Pasquali, C.L. Hill, Polyoxometalate systems for the catalytic selective production of nonthermodynamic alkenes from alkanes. Nature of excited-state deactivation processes and control of subsequent thermal processes in polyoxometalate photoredox chemistry, J. Am. Chem. Soc. 112 (1990) 6585-6594.

[74] H.J. Kuhn, S.E. Braslavsky, R. Schmidt, Chemical actinometry (IUPAC Technical Report), Pure Appl. Chem. 76 (2004) 2105–2146.

[75] K. Nomiya, Y. Sugie, K. Amimoto, M. Miwa, Charge-transfer absorption spectra of some tungsten(VI) and molybdenum(VI) polyoxoanions, Polyhedron, 6 (1987) 519-524.

[76] D. Ravelli, D. Dondi, M. Fagnoni, A. Albini, A. Bagno, Electronic and EPR spectra of the species involved in $[W_{10}O_{32}]^{4-}$ photocatalysis. A relativistic DFT investigation, Phys. Chem. Chem. Phys. 15 (2013) 2890-2896.

[77] E.S. Da Silva, P. Wong-Wah-Chung, M. Sarakha, H.D. Burrows, Photophysical characterization of the plant growth regulator 2-(1-naphthyl) acetamide, J. Photochem. Photobiol. A: Chem. 265 (2013) 29-40.

[78] M. Montalti, A. Credi, L. Prodi, M.T. Gandolfi, Handbook of Photochemistry, Third edition ed., CRC Press, Taylor & Francis Group, Boca Raton, Florida, 2006.

[79] C. Giannotti, C. Richter, Photocatalysed oxidation of cyclohexane by $W_{10}O_{32}^{4-}$ irradiation with natural sunlight, Int. J. Photoenergy 1 (1999) 1-5.

[80] I.N. Lykakis, C. Tanielian, R. Seghrouchni, M. Orfanopoulos, Mechanism of decatungstate photocatalyzed oxygenation of aromatic alcohols: Part II. Kinetic isotope effects studies, J. Mol. Catal. A: Chem. 262 (2007) 176-184.

[81] C. Tanielian, I.N. Lykakis, R. Seghrouchni, F. Cougnon, M. Orfanopoulos, Mechanism of decatungstate photocatalyzed oxygenation of aromatic alcohols: Part I. Continuous photolysis and laser flash photolysis studies, J. Mol. Catal. A: Chem. 262 (2007) 170-175.

[82] T.D. Bucheli, O.P. Haefliger, R. Dietiker, R. Zenobi, Analysis of Water Contaminants and Natural Water Samples Using Two-Step Laser Mass Spectrometry, Anal. Chem. 72 (2000) 3671-3677.

[83] X. Esparza, E. Moyano, J.R. Cosialls, M.T. Galceran, Determination of naphthalene-derived compounds in apples by ultra-high performance liquid chromatography-tandem mass spectrometry, Anal. Chim. Acta 782 (2013) 28-36.

[84] M.J. Climent, M.A. Miranda, Photodegradation of Dichlorprop and 2-Naphthoxyacetic Acid in Water. Combined GC−MS and GC−FTIR Study, J. Agric. Food Chem. 45 (1997) 1916-1919.

[85] M.J. García-Martínez, L. Canoira, G. Blázquez, I. Da Riva, R. Alcántara, J.F. Llamas, Continuous photodegradation of naphthalene in water catalyzed by TiO_2 supported on glass Raschig rings, Chem. Eng. J. 110 (2005) 123-128.

[86] L. Hykrdová, J.r. Jirkovský, G. Mailhot, M. Bolte, Fe(III) photoinduced and Q-TiO_2 photocatalysed degradation of naphthalene: comparison of kinetics and proposal of mechanism, J. Photochem. Photobiol. A: Chem. 151 (2002) 181-193.

[87] A. Lair, C. Ferronato, J.-M. Chovelon, J.-M. Herrmann, Naphthalene degradation in water by heterogeneous photocatalysis: An investigation of the influence of inorganic anions, J. Photochem. Photobiol. A: Chem. 193 (2008) 193-203.

[88] B.J. McConkey, L.M. Hewitt, D.G. Dixon, B.M. Greenberg, Natural Sunlight Induced Photooxidation of Naphthalene in Aqueous Solution, Water, Air, and Soil Pollut. 136 (2002) 347-359.

[89] E. Pramauro, A.B. Prevot, M. Vincenti, R. Gamberini, Photocatalytic degradation of naphthalene in aqueous TiO_2 dispersions: Effect of nonionic surfactants, Chemosphere, 36 (1998) 1523-1542.

[90] D. Vialaton, C. Richard, D. Baglio, A.-B. Paya-Perez, Mechanism of the photochemical transformation of naphthalene in water, J. Photochem. Photobiol. A: Chem. 123 (1999) 15-19.

[91] T. Kothe, R. Martschke, H. Fischer, Photoreactions of the decatungstate anion $W_{10}O_{32}^{4-}$ with organic substrates in solution studied by EPR and kinetic absorption spectroscopy: an example for the persistent radical effect, J. Chem. Soc., Perkin Trans. 2 (1998) 503-508.

[92] A. Chemseddine, C. Sanchez, J. Livage, J.P. Launay, M. Fournier, Electrochemical and photochemical reduction of decatungstate: a reinvestigation, Inorg. Chem. 23 (1984) 2609-2613.

Figure Captions

Fig. 1. UV absorption spectra of $W_{10}O_{32}^{4-}$ (3.0×10^{-4} mol L^{-1}) (dotted line) and of NAD (3.0×10^{-4} mol L^{-1}) (solid line) in aqueous solution. The chemical structure of NAD as well as the emission spectra of solar light (■) are also given.

Fig. 2. Kinetics of NAD (3.0×10^{-4} mol L^{-1}) degradation in aerated aqueous solution irradiated with the Suntest in: (◆) presence and (Δ) absence of $W_{10}O_{32}^{4-}$ (3.0×10^{-4} mol L^{-1}) at pH 5.0 obtained by LC-DAD ($\lambda_{det} = 280$ nm).

Fig. 3. Evolution of NAD (3.0×10^{-4} mol L^{-1}) disappearance in aqueous solution: i) (○) in aerated conditions and absence of $W_{10}O_{32}^{4-}$; ii) in presence of $W_{10}O_{32}^{4-}$ (3.0×10^{-4} mol L^{-1}) in: (■) de-aerated, (●) aerated and (☆) oxygenated conditions; and iii) (✳) in presence of $W_{10}O_{32}^{4-}$ (3.0×10^{-4} mol L^{-1}) and *iso*-propanol (1.0 mol L^{-1}) under aerated conditions. Irradiation at 365 nm and $\lambda_{det} = 280$ nm.

Fig. 4. TOC (○) and nitrates (☆) evolution profile of aerated aqueous NAD solution (3.0×10^{-4} mol L^{-1}) irradiated at 365 nm in the presence of $W_{10}O_{32}^{4-}$ (3.0×10^{-4} mol L^{-1}), as a function of irradiation time.

Fig. 5. LC-DAD-ES$^+$/MS chromatogram of aerated aqueous solution of the mixture [NAD (3.0×10^{-4} mol L^{-1}) + $W_{10}O_{32}^{4-}$ (3.0×10^{-4} mol L^{-1})] (2 h irradiation, $\lambda_{det} = 250$ nm).

Fig. 6. MS^2 spectrum for the product with $m/z = 218$.

Fig. 7. MS^2 spectrum for the product with $m/z = 232$.

Scheme 1. General scheme of NAD hydrolysis into 1-NAA, NH_3 (and NH_4^+).

Scheme 2. Proposed mechanism for the degradation of NAD photocatalysed by $W_{10}O_{32}^{4-}$ in aqueous solution.
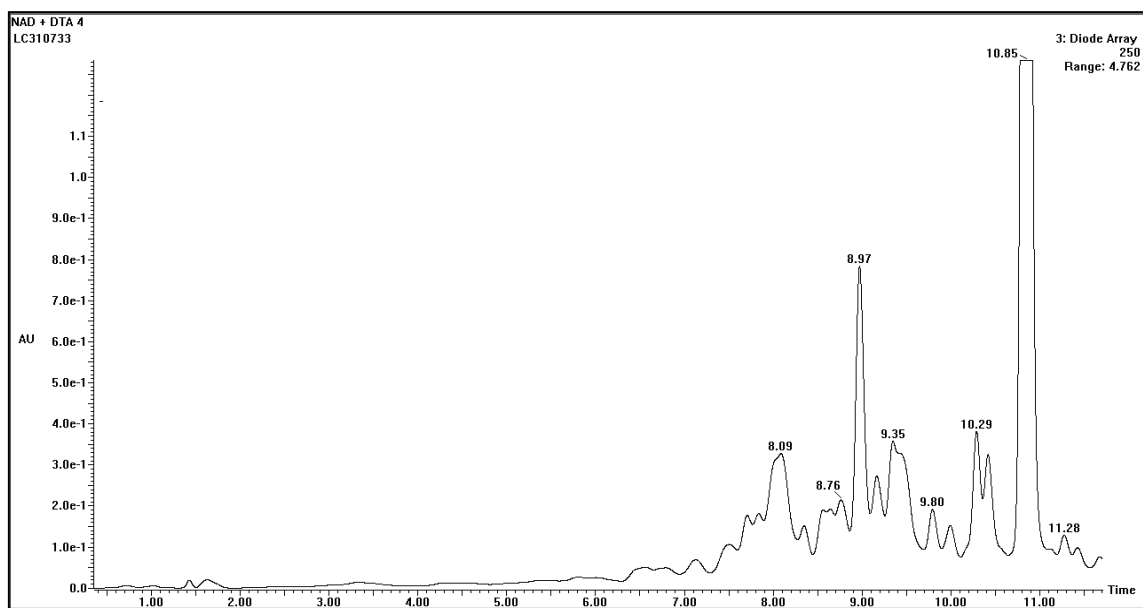
FIGURE.1
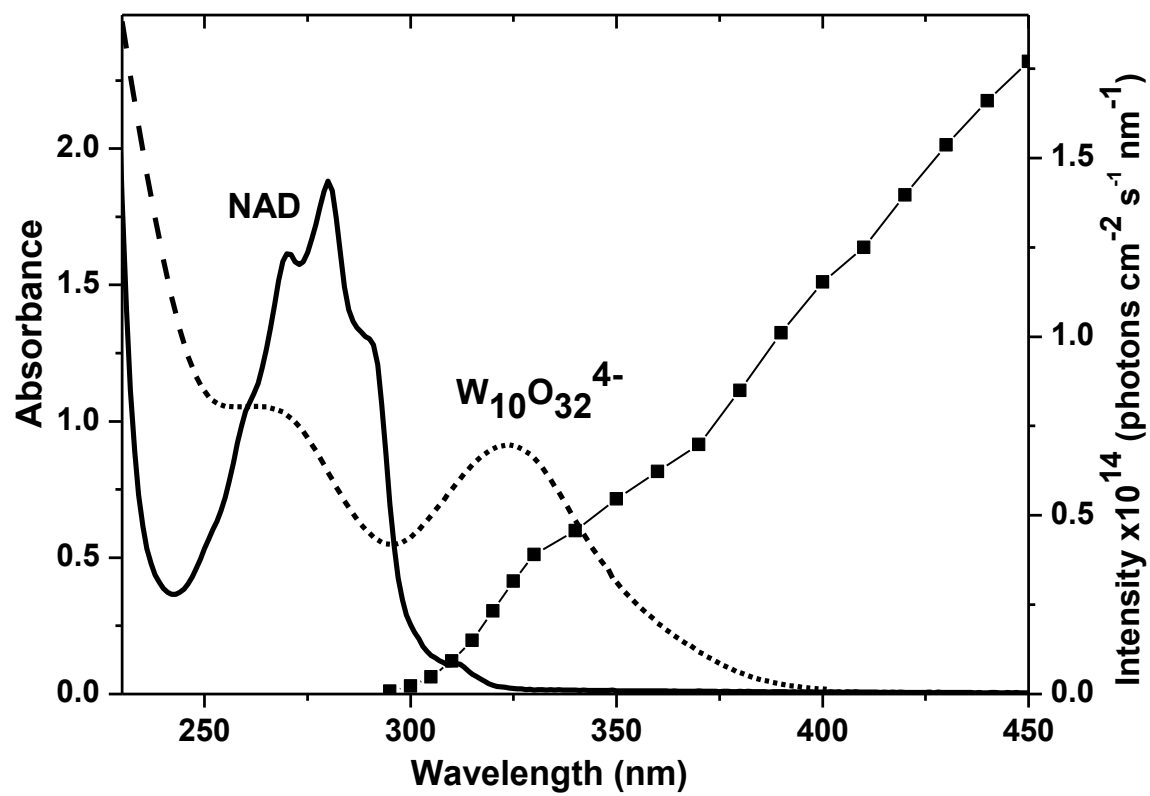
FIGURE.2
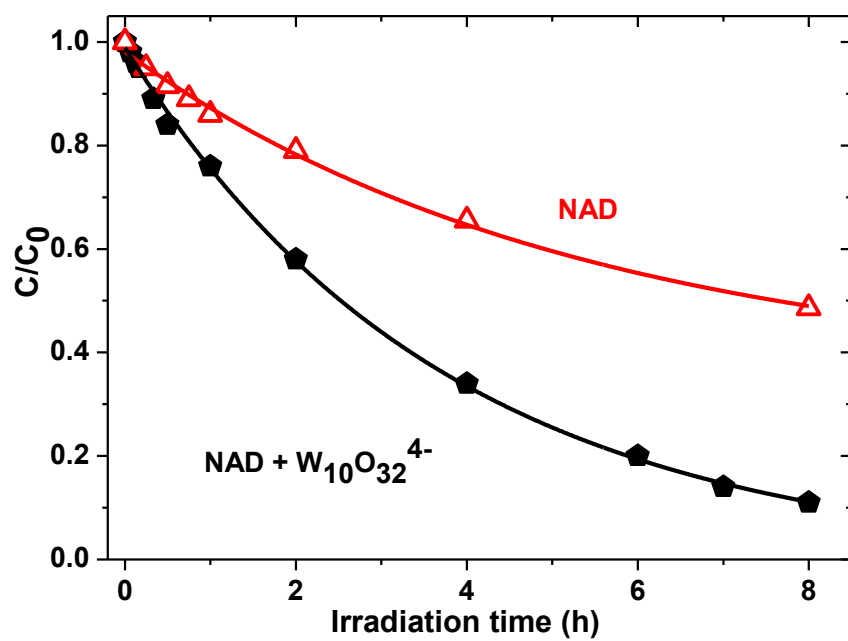
FIGURE.3
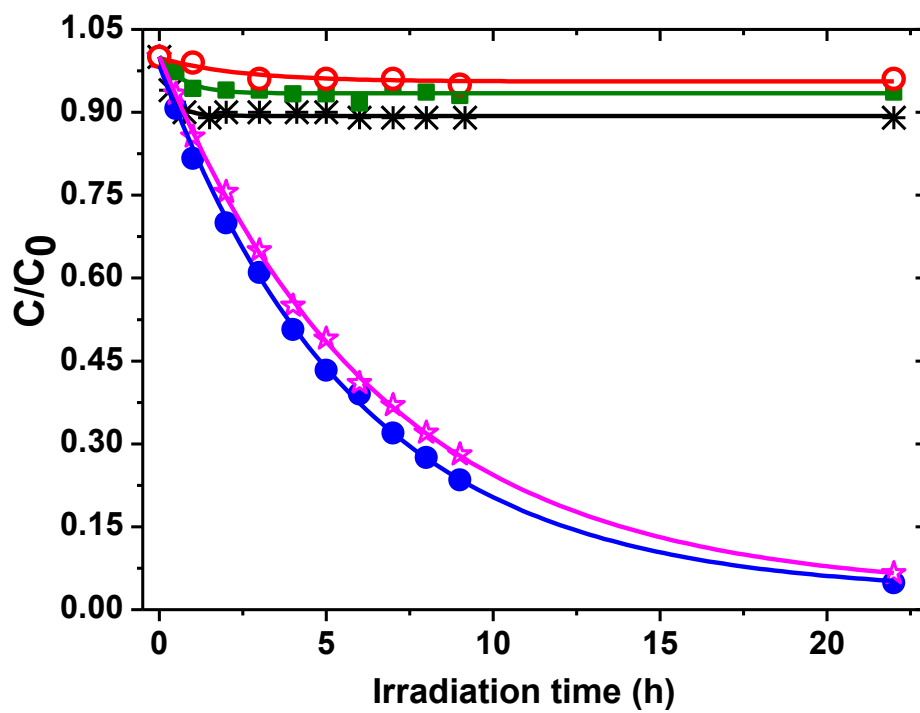
FIGURE.4
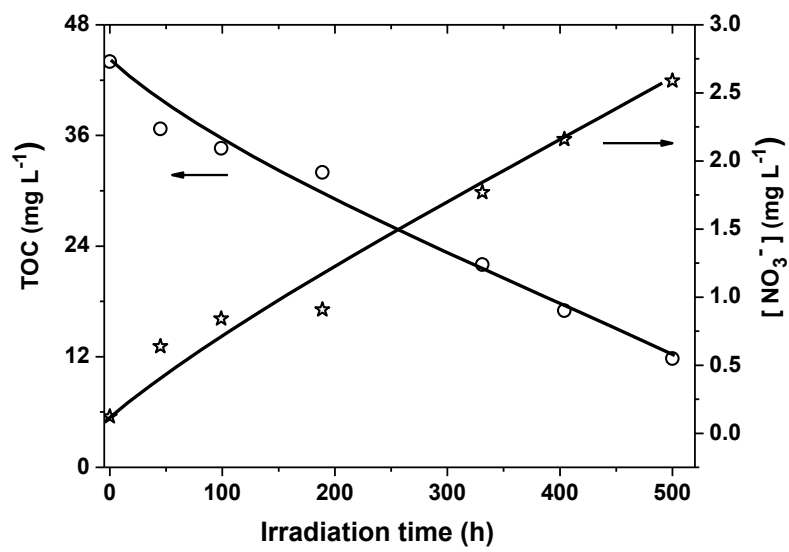
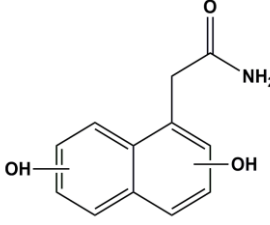FIGURE.5

FIGURE.6
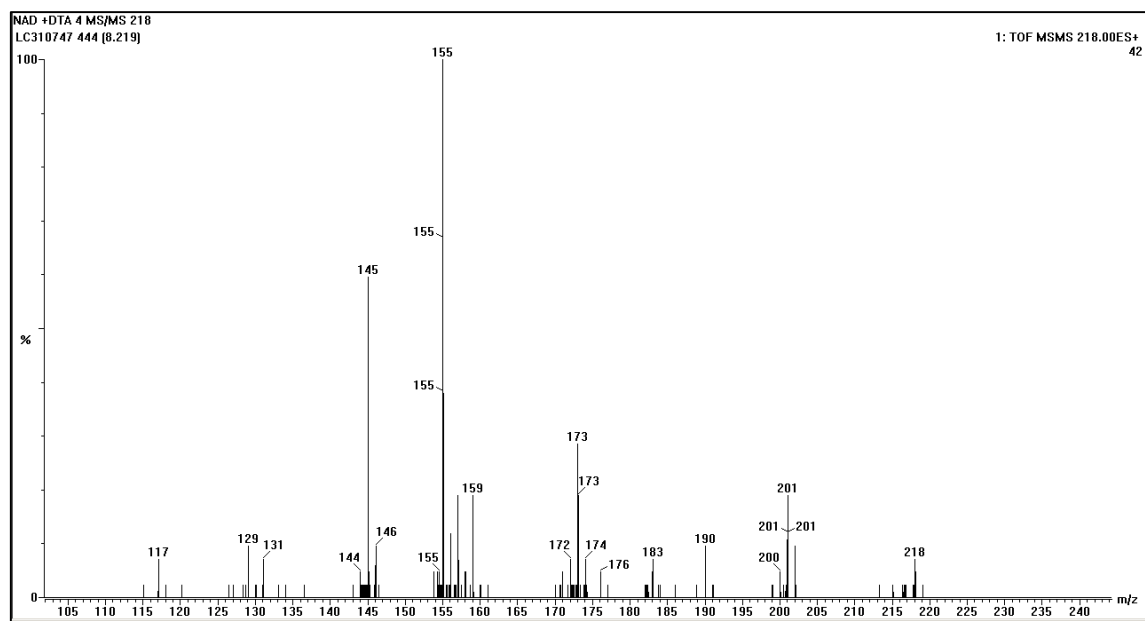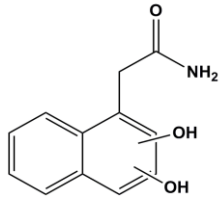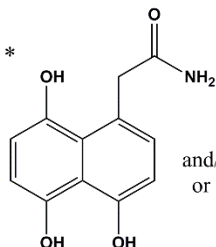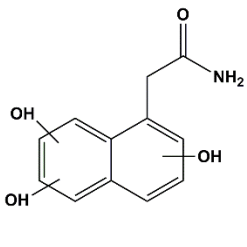
FIGURE.7
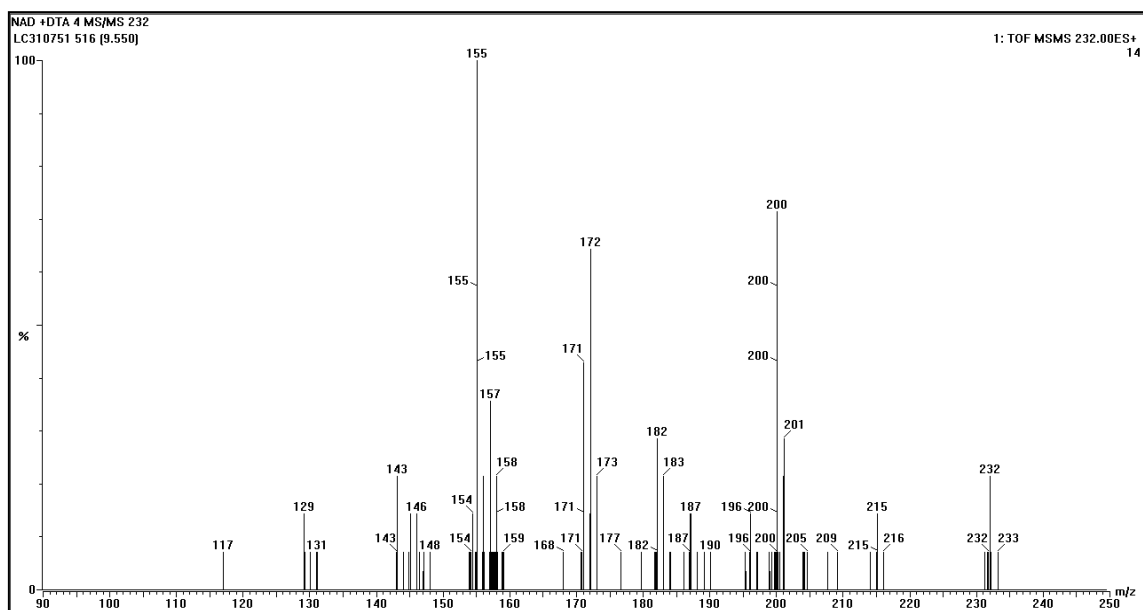
SCHEME.1

SCHEME.2
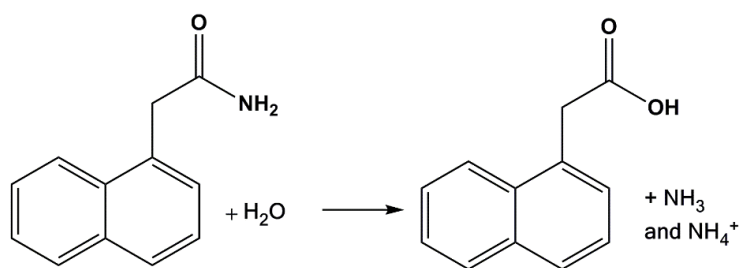
Table 1. Initial rate constants (k), half-lives ($t_{1/2}$) and quantum yields (ϕ) of NAD (3.0×10^{-4} mol L^{-1}) degradation in aqueous solution in presence of the catalyst $W_{10}O_{32}{}^{4-}$ (3.0×10^{-4} mol L^{-1}) irradiated under different oxygen concentrations [78].

Conditions	$[O_2]$ (20°C) (mol L^{-1})	k ($\times10^{-3}$ min^{-1})	$t_{1/2}$ (h)	ϕ_{NAD} ($\times10^{-3}$)*
Aerated	2.9×10^{-4}	3.2 ± 0.3	3.6 ± 0.3	1.9 ± 0.2
Oxygenated	1.39×10^{-3}	2.3 ± 0.3	5.0 ± 0.6	1.3 ± 0.2
De-aerated	$< 10^{-5}$	-	-	0.8 ± 0.1

* monochromatic light at 365 nm

Table 2. Retention time (t_{ret}), parent molecular and main fragments ion, UV data and proposed structure of some NAD photoproducts obtained by LC-MS/MS-ES[+]. UV absorption data were obtained by coupling DAD. ([*] most stable structure; [a] shoulder).

t_{ret} (min)	Main fragments m/z (% abundance)	λ_{max} (nm)	Proposed chemical structure
10.8	[M+H]$^+$ =186 (15%), 169 (10%), 141 (100%)	280	(NAD)
11.3	-	280	(1-NAA)
10.3	[M+H]$^+$ = 202 (100%), 185 (50%), 157 (15%), 143 (10%)	290	
9.4	[M+H]$^+$ = 202 (100%), 184 (30%), 156 (20%)	280	
8.8	[M+H]$^+$ = 216 (40%), 199 (30%), 171 (60%), 143 (100%)	240, 330	
6.8	[M+H]$^+$ = 232 (50%), 214 (15%), 200 (100%), 172 (75%), 155 (50%)	265, 320	
9.5	[M+H]$^+$ = 232 (20%), 216 (5%), 200 (71%), 172 (63%), 155 (100%)	275, 340	
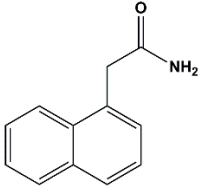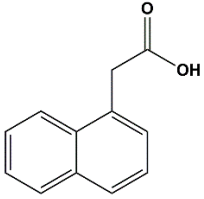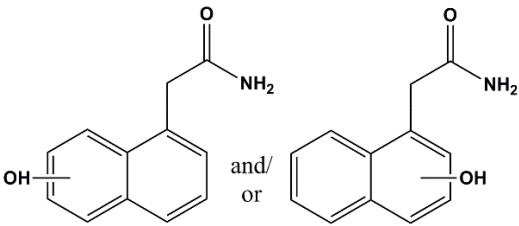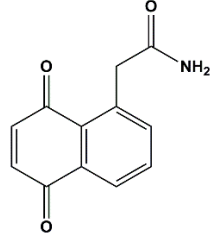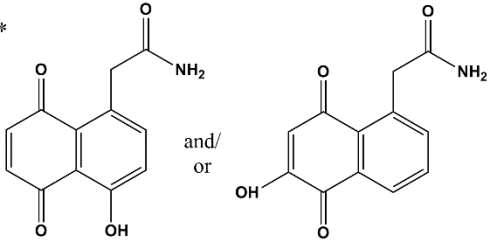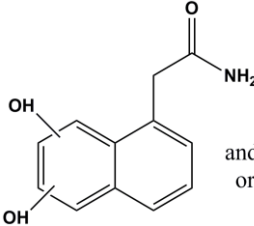
7.8	[M+H]$^+$ = 218 (25%), 201 (30%), 173 (50%), 155 (100%)	248, 290	
8.2 6.6	[M+H]$^+$ = 218 (8.0%), 201 (20%), 173 (28%), 155 (100%)	252, 290	
8.6	[M+H]$^+$ = 218 (5.%), 201 (20%), 173 (30%), 155 (100%)	290	
9.0	[M+H]$^+$ = 218 (5.0%), 200 (20%), 182 (100%), 154 (20%)	231, 280[a], 300	
7.4	[M+H]$^+$ = 218 (15.0%), 200 (40%), 182 (100%), 154 (30%)	252, 285[a]	
	[M+H]$^+$ = 218 (10%), 200 (20%), 172 (100%), 155 (35%)	260	
7.1	[M+H]$^+$ = 234 (10%), 216 (100%), 188 (35%), 171 (60%), 157 (10%)	234	
6.0	[M+H]$^+$ = 234 (10%), 216 (100%), 198 (55%), 170 (10%), 153 (10%)	232, 300[a]	